Monte Carlo Approach to the Analysis of the Rotational Diffusion of Wormlike Chains

PAUL J. HAGERMAN, *Department of Biochemistry, Biophysics and Genetics, University of Colorado Medical Center, Denver, Colorado 80262;* and BRUNO H. ZIMM, *Department of Chemistry, University of California, San Diego, La Jolla, California 92093*

Synopsis

A Monte Carlo analysis is presented which establishes a relationship between the rotational diffusion coefficients and the flexibility (persistence length, P) of short, wormlike chains. The results of this analysis are presented in terms of experimentally observable quantities; namely, the rotational relaxation times for the field-free decay of optical anisotropy. The pertinent theoretical quantity is R, defined as the ratio of the longest rotational relaxation time of a wormlike chain to the transverse rotational relaxation time of a rigid cylinder having the same axial length (L) and segmental volume. R, so defined, is essentially independent of the axial ratio of the cylinder for any value of L/P within the range of validity of the present analysis (axial ratio > 20; $0.1 < L/P < 5$). It is pointed out that P can be determined with reasonable accuracy even in the absence of a precise knowledge of the local hydrodynamic radius of the chain.

INTRODUCTION

It has been known for some time that the behavior of an elongated particle undergoing rotational diffusion is extremely sensitive to the axial length of the particle. Theoretical studies[1–4] all suggest that the transverse (smallest) rotational diffusion coefficient is roughly proportional to the inverse cube of the length. These theoretical observations (particularly those of Broersma[4]) have gained experimental support from studies of the rotational diffusion of tobacco mosaic virus (TMV)[5–7] and short fragments of DNA[8–10] using transient electric birefringence or dichroism (TEB or TED, respectively). The studies of DNA have further demonstrated that as the fragment length is increased, the rotational relaxation times (the observable quantities related to the diffusion coefficients) become substantially smaller than those predicted on the basis of expected rigid-rod behavior. It has been suggested[8] that this difference is due to the internal flexibility of DNA.

The major objective of this paper is to establish a quantitative relationship between the longest rotational relaxation time of a linear polymer of a given axial length (L) and the flexibility (persistence length, P) of the polymer. The extreme sensitivity of these relaxation times to the axial length, for rigid rodlike molecules, suggests that the study of weakly to

Biopolymers, Vol. 20, 1481–1502 (1981)

CCC 0006-3525/81/071481-22$02.20

moderately flexible molecules ($L/P < 5$) would provide a more precise estimate of the persistence length than can be obtained through conventional means such as sedimentation or light scattering. Moreover, such short molecules would not be influenced significantly by excluded-volume effects,[11] thus enabling experimental studies to be carried out with polyelectrolytes under conditions of very low ionic strength.

Hearst[12] has presented an analysis of the rotational diffusion of wormlike chains, which contained several simplifying assumptions now known to lead to significant inaccuracy. In particular, it was assumed that the hydrodynamic interactions among elements of an individual chain could be preaveraged over configuration space and that the sums over the pairwise interactions between elements of the chain could be adequately represented by integrals. These assumptions will be discussed in more detail below; however, despite the approximate nature of Hearst's approach, his results have proven to be useful in carrying out the present study.

The present analysis of the rotational diffusion of flexible polymers is based on the representation of these polymers by isotropically bendable wormlike chains, and the computational approach is comprised of three parts; namely, (1) the generation by a random-number program of ensembles of wormlike chains having specified contour lengths (L) and persistence lengths (P), (2) the computation of the principal rotational diffusion coefficients about the center of frictional resistance (CFR), and (3) the determination of the observable quantities (rotational relaxation times) for each system, based on the equilibrium-ensemble approach. The current ("Monte Carlo") approach is necessitated, since, as has been shown by Zimm,[13] configurational preaveraging can lead to substantial errors in the evaluation of the hydrodynamic properties of flexible polymers.

It will also be shown that information pertaining to chain flexibility can be extracted from rotational relaxation times in the absence of a precise knowledge of the local hydrodynamic radius of the molecule. Therefore, the following analysis should be applicable to a wide variety of linear polymers, provided that the lengths of the polymers are known with reasonable precision; and even in the absence of precise information concerning length, changes in flexibility and/or local polymer conformation can be studied. In the accompanying article,[11] the results of this analysis have been applied to the study of the ionic-strength dependence of the flexibility of DNA.

ANALYTICAL APPROACH

Hydrodynamic Model for an Individual Wormlike Chain

The model employed in the present analysis consists of a chain of touching beads (Stokes' spheres), where N beads are joined by $N - 1$ segments, and where the length of an equivalent cylinder is determined by $L(\text{cylinder}) = 2\sigma(N - 1)$; σ is the hydrodynamic radius of an individual

bead. For a summary of the features of the model, see Fig. 1. In order to compare the results of the present analysis of the rotational diffusion of wormlike chains to the limiting behavior as $P \rightarrow \infty$, the hydrodynamic properties of the linear string of beads will be compared to a volume-adjusted, continuous-cylinder model of radius b, where $b(\text{cylinder}) = (2/3)^{1/2}\sigma$. As an example, for $b(\text{DNA}) = 13$ Å, $\sigma = 15.9$ Å, and the bead spacing (l) would be 9.4 base pairs (bp) (assuming 3.4 Å/bp). For the case of touching beads, $l = 2\sigma$. This choice is based in part on the work of Garcia de la Torre and Bloomfield,[14] who observed that bead representations of ellipsoids of revolution have frictional properties which are in close agreement with those of the ellipsoid when the volumes of the two subjects are equal. Moreover, as will be seen below, the rotational diffusion coefficients of the volume-adjusted bead and cylinder models agree to within a few percent; however, as will be shown later in this article, the final results are rather insensitive to the precise bead spacing and hydrodynamic radius.

Furthermore, it is assumed that there is no preferred axis of bending between segments (isotropic-ϕ model[15]); that is, for a given latitudinal angle (θ_i), the longitudinal angle (ϕ_i) may assume any value between 0 and 2π radians with equal probability. In addition, the standard assumption of a free energy of bending, quadratic in θ_i (representing a restoring force linear in the angular displacement), has been invoked, leading to a proba-

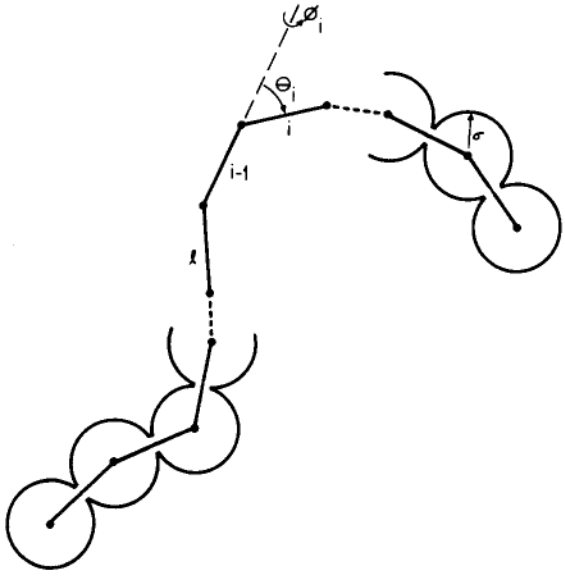

Fig. 1. Model for the wormlike chain used for the determination of rotational diffusion coefficients. The longitudinal angles (ϕ_i) and latitudinal angles (θ_i) are as specified in the text for the isotropic-ϕ model (Ref. 15). The interbead spacing (l) is twice the hydrodynamic radius (σ) (touching-bead model). The beads are centered at the ends of each segment; therefore, for a chain composed of $N - 1$ segments, there are N beads.

bility distribution function (F) for θ_i given by Ref. 15:

$$F(\theta_i) = C \exp(-a\theta_i^2/2) \sin \theta_i \tag{1}$$

where C is a normalization constant, and where the bending force constant divided by kT is given by

$$a = P/l \tag{2}$$

Solution of the Hydrodynamic Problem for Rotational Diffusion of Wormlike Chains

The following analysis is based on the formalism of Kirkwood[16–18] as extended by Yamakawa,[19] Garcia de la Torre and Bloomfield,[14,20] and Zimm.[13] It is assumed that the wormlike chain is experiencing pure rotational motion; that is, its CFR is at rest in the unperturbed fluid (see Results and Discussion). The relative velocity (V_i) of the ith bead with respect to the local fluid is given by

$$\mathbf{V}_i = \boldsymbol{\omega} \times \mathbf{r}_i - \mathbf{v}_i \tag{3}$$

where $\boldsymbol{\omega}$ is the angular velocity of the chain about its CFR, $\mathbf{r}_i$ is the position of the ith bead with respect to the CFR, and $\mathbf{v}_i$ represents the velocity of the fluid at the position of the ith bead due to the motions of the remaining $N - 1$ beads, but with bead i absent. In the formalism of Kirkwood, the velocity perturbation is given by

$$\mathbf{v}_i = \sum_j \mathbf{T}_{ij} \cdot \mathbf{F}_j \qquad (j \neq i) \tag{4}$$

where

$$\mathbf{T}_{ij} = (8\pi\eta_0 R_{ij})^{-1} \left[\left(\mathbf{I} + \frac{\mathbf{R}_{ij}\mathbf{R}_{ij}}{R_{ij}^2}\right) - \frac{2\sigma}{R_{ij}}\left(\frac{1}{3}\mathbf{I} - \frac{\mathbf{R}_{ij}\mathbf{R}_{ij}}{R_{ij}^2}\right)\right] \tag{5}$$

Equation (5) (Eq. (21) of Ref. 19) is a modified version of the Oseen-Burgers hydrodynamic interaction tensor,[3] which introduces a first-order correction for finite bead volume. $\mathbf{R}_{ij}$ represents the vectorial separation between the centers of the ith and jth beads, and σ represents the radius of the individual beads in the chain.

In general, for molecules lacking three-fold symmetry, the CFR must be entered as an unknown into the set of coupled hydrodynamic equations for rotation. This can be done conveniently in the following manner. If $\mathbf{r}_{i,0}$ is the position of the ith bead with respect to an arbitrarily chosen origin, then

$$\mathbf{r}_{i,0} = \mathbf{r}_i + \mathbf{R}_0 \tag{6}$$

where $\mathbf{R}_0$ is the position of the CFR relative to the origin (all vectorial quantities are referred to the frame in which the unperturbed fluid is at rest). It follows that

$$\boldsymbol{\omega} \times \mathbf{r}_{i,0} = \boldsymbol{\omega} \times \mathbf{r}_i + \boldsymbol{\omega} \times \mathbf{R}_0 \tag{7}$$

and therefore that

$$\mathbf{V}_i = -\boldsymbol{\omega} \times \mathbf{R}_0 + \boldsymbol{\omega} \times \mathbf{r}_{i,0} - \mathbf{v}_i \tag{8}$$

The frictional force exerted on the fluid by each bead is given by

$$\mathbf{F}_i = \rho \mathbf{V}_i = \rho(\mathbf{u} + \boldsymbol{\omega} \times \mathbf{r}_{i,0} - \mathbf{v}_i) \tag{9}$$

where ρ is the frictional resistance for translation of a Stokes' sphere ($\rho = 6\pi\eta_0\sigma$) and where $\mathbf{u}$ ($= -\boldsymbol{\omega} \times \mathbf{R}_0$) is the velocity of the arbitrary origin with respect to the CFR. Thus, by including three additional unknowns (the components of $\mathbf{u}$), one can solve for the component forces with respect to the CFR.

There are now $3N + 3$ unknowns: the $3N$ component forces $\mathbf{F}_{i,\alpha}$ ($\alpha = x, y, z$) as well as the components of $\mathbf{u}$. Equation (9) provides $3N$ expressions relating the unknown quantities, and the 3 additional relations,

$$\sum_i \mathbf{F}_{i,\alpha} = 0 \qquad (\alpha = x, y, z) \tag{10}$$

are provided by the fact that there is no net force applied to the rotating chain (i.e., the CFR is stationary in the unperturbed fluid). The component forces can be determined by solving the set of coupled equations [Eqs. (9) and (10)] exactly by numerical procedures, provided that N is less than 100. For larger values of N, computation times become prohibitive, and one must resort to alternative approaches such as the iterative method described by Garcia de la Torre and Bloomfield.[14,20]

The total torque ($\mathbf{T}$) acting on the chain is given by

$$\mathbf{T} = \boldsymbol{\zeta} \cdot \boldsymbol{\omega} = \sum \mathbf{r}_i \times \mathbf{F}_i = \sum \mathbf{r}_{i,0} \times \mathbf{F}_i \tag{11}$$

where $\boldsymbol{\zeta}$ is the friction tensor for pure rotation. It should be noted that

$$\mathbf{R}_0 \times \sum_i \mathbf{F}_i = 0$$

by Eq. (10). Diagonalization of $\boldsymbol{\zeta}$ yields three principal diffusion coefficients through the Einstein relations:

$$\zeta_p = kT/D_p \qquad (p = 1, 2, 3) \tag{12}$$

Approximate Solution of the Hydrodynamic Problem for Rotational Diffusion

Using the formalism of Kirkwood, Hearst[12] derived an expression for the smallest rotational diffusion coefficient of a wormlike chain. Yamakawa and Yamaki[21] have discussed the approximations implicit in Kirkwood's approach, and those authors have pointed out that Kirkwood's results are only correct when the frictional force exerted by each bead is proportional to the distance of that bead from the axis of rotation. Yamakawa and Yamaki have shown also that for rotational diffusion of linear assemblies of identical beads, the above condition of proportionality is

satisfied; hence, Hearst's equation becomes exact in the rigid-rod limit, and for long, thin rods, becomes identical in form to the continuous cylinder model.[3,4] Garcia de la Torre and Bloomfield[20] further demonstrated that Hearst's diffusion equation could be reproduced as a first-order approximation to the true solution for an arbitrary arrangement of beads. This approximate expression is given by

$$D_{\hat{z}} = \left(\frac{kT}{\rho S_{\hat{z}}}\right)\left[1 + \left(\frac{3\sigma}{4S_{\hat{z}}}\right)\sum_i \sum_{j\neq i}\left(\frac{x_i x_j - y_i y_j}{R_{ij}} - \frac{(x_i y_j - x_j y_i)^2}{R_{ij}^3}\right)\right] \tag{13}$$

(for rotation about the $\hat{z}$ axis), where

$$S_{\hat{z}} = \sum_i (x_i^2 + y_i^2)$$

Since Eq. (13) approaches the exact solution in the limit of completely rigid (linear) chains as $N \to \infty$, it should serve as a reasonable, approximate solution for the rotational diffusion coefficients of short, wormlike chains. Therefore, as a computational expedient, Eq. (13) will be used to solve (approximately) for the principal diffusion coefficients for each chain ($D_{\hat{\alpha}}$; $\hat{\alpha} = \hat{x}, \hat{y}, \hat{z}$) by employing the center of mass as an approximate CFR and using the axes that diagonalize the inertia tensor as $\hat{x}, \hat{y}, \hat{z}$. The axes $\hat{x}, \hat{y}, \hat{z}$ are not, in general, equal to the principal axes of the friction tensor. The values of the $D_{\hat{\alpha}}$ so obtained will be corrected subsequently by comparison with the formal approach described below, thus yielding a corrected set of rotational diffusion coefficients. This approach, which involves the application of a correction term to the approximate solution, is based on the observation that while the variation among the values of D, computed for a given set of chains, may be large (by either method), the difference between $D_{\hat{\alpha}}$ and D_p on a chain-by-chain basis does not vary widely; this allows the use of a more restricted (and hence computationally feasible) set of chains for the solution of Eqs. (9) and (10).

Determination of the Macroscopic, Rotational Relaxation Times for the Field-Free Decay of Induced Optical Anisotropy

At this point, the analysis of the rotational diffusion of wormlike chains will be described in terms of observable quantities; namely, the rotational relaxation times (τ), since the D_p are not directly observable. The main assumption employed in the current analysis is that local, segmental motions occur more rapidly than does overall rotational diffusion (discussed later in this article), thus allowing the description of the rotational diffusion of a wormlike chain in terms of ensemble-averaged quantities $\langle D_p \rangle$.

The decay of optical anisotropy accompanying the rotational diffusion of a rigid particle of arbitrary shape can be described in general in terms of five relaxation times.[22] These relaxation times are identical to the five relaxation times used to describe the decay of fluorescence polarization.[23–25] An earlier analysis of the decay of birefringence[26,27] yielded only two re-

TABLE I
Rotational Relaxation Times for a Rigid Particle[a]

i	$1/\tau_i$	
	$D_1 \neq D_2 \neq D_3$	$D_1 = D_2 \neq D_3$
1	$6D - 2B$[b]	$6D_1$
2	$3(D + D_1)$	$5D_1 + D_3$
3	$3(D + D_2)$	$5D_1 + D_3$
4	$3(D + D_3)$	$2D_1 + 4D_3$
5	$6D + 2B$	$2D_1 + 4D_3$

[a] Tabulated in Ref. 22.
[b] $D = (1/3)(D_1 + D_2 + D_3)$; $B = (D_1^2 + D_2^2 + D_3^2 - D_1D_2 - D_2D_3 - D_1D_3)^{1/2}$.

laxation times; however, that analysis contained certain restrictions on the symmetry of the particle.[22] In Table 1 I, the relaxation times have been expressed in terms of the three principal rotational diffusion coefficients. When two of the diffusion coefficients are equal, as in the case of particles having cylindrical symmetry, the number of nondegenerate relaxation times is reduced to three, and the longest relaxation time $\tau = 1/3(D_1 + D_2) = 1/6D_1$ $(D_1 = D_2 < D_3)$ corresponds to the classical result[2,28]; namely, that for ellipsoids of revolution, $\tau = 1/6D$(transverse). It should also be noted that τ_1 is independent of D_3 for this special case.

For wormlike coils having $L/P < 5$, $\langle D_2 \rangle / \langle D_1 \rangle < 1.1$ and $\langle D_3 \rangle > 5 \langle D_2 \rangle$; and as a consequence,

$$1/\tau_1 = 3(\langle D_1 \rangle + \langle D_2 \rangle) \tag{14}$$

to within 0.1%. Moreover, the remaining relaxation times are all coupled to the largest diffusion coefficient (D_3), corresponding to rotation about the longitudinal axis in the rigid-rod limit. This coupling results in an effective separation between τ_1 and τ_{2-5} for relatively short chains; however, as L/P is increased beyond ~5, τ_1 and the collection (τ_{2-5}) approach each other to within a factor f 2, thus limiting the practical range of this analysis if the amplitudes associated with the more rapid relaxation times are appreciable (for further discussion of this point, see the following paper[11]).

METHODS OF COMPUTATION

Angle Generators for θ_i and ϕ_i

As described above, the spatial configuration of each chain is determined by an ordered set of θ_i and ϕ_i angles which are generated according to the requirements of the model (i.e., segment length, persistence length, bending potential). For the present analysis, the ϕ_i are assumed to be isotropic and are generated by the numerical algorithm

$$\phi_i = 2\pi \text{ RANDOM} \tag{15}$$

where RANDOM is a standard ALGOL pseudo-random-number generator with output values distributed between 0 and 1. The latitudinal angles (θ_i) are generated by successive application of two orthogonal angular displacements ($\theta_{i,1}$ and $\theta_{i,2}$) in the x-y and x-z planes of the $(i-1)$st frame [the x axis in the $(i-1)$st frame corresponds to $\theta_i = 0$], the expression for θ_i being given by

$$\theta_i \cong (\theta_{i,1}^2 + \theta_{i,2}^2)^{1/2} \tag{16}$$

for $\theta_i < 1$ radian. The component angles ($\theta_{i,j}$) are normally distributed about $\theta_{i,j} = 0$ with a standard deviation of $(l/P)^{1/2}$.[15] The resultant (approximate) distribution function for θ_i is given by

$$F'(\theta_i) = C' \exp(-a\theta_i^2/2)\theta_i \tag{17}$$

Figure 2 shows a comparison of a set of computed θ_i with the curve predicted by Eq. (1). The $\theta_{i,j}$ are generated by the ALGOL intrinsic NORRF4, which produces normally distributed random numbers using linear congruential generators.[29]

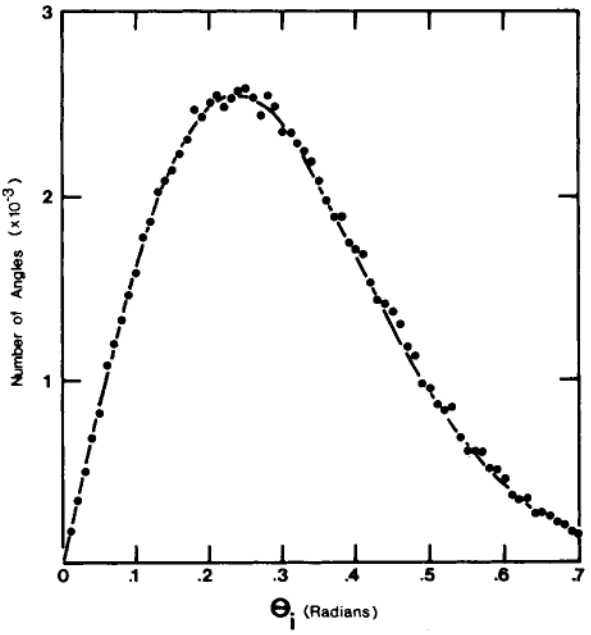

Fig. 2. Comparison of the distribution of a set of 10^5 latitudinal angles (θ_i) with the theoretical probability distribution function for the isotropic-ϕ model. The filled circles represent accumulated θ_i values in 0.01-radian annular regions with the accumulated values represented at the midpoint of the annulus. The solid line represents the predicted angular dependence [Eq. (1)]. This computation was carried out for $P = 600$ Å, $\sigma = 17$ Å.

Generation of Individual Chains

The configuration of the collection of segment vectors comprising an individual chain is generated by successive application of a transformation matrix $(\mathbf{A}_i)$[30] given by

$$\mathbf{A}_i = \begin{bmatrix} \cos\theta_i & -\sin\theta_i & 0 \\ \sin\theta_i \cos\phi_i & \cos\theta_i \cos\phi_i & -\sin\phi_i \\ \sin\theta_i \sin\phi_i & \cos\theta_i \sin\phi_i & \cos\phi_i \end{bmatrix} \tag{18}$$

(A_{21} was misprinted in the original reference.) $\mathbf{A}_i$, when applied to the components of a vector in the local coordinates of the ith segment, transforms it to the $(i-1)$st coordinate frame. As a computational check of the overall chain-generation procedure, computed values of $\langle h^2\rangle/L^2$ (reduced, mean-squared, end-to-end distance) for ensembles of chains having various values of L and P have been compared (Fig. 3) with the values predicted by the well-known expression

$$\langle h^2\rangle/L^2 = (2P/L)\,[1 - P/L + (P/L)\exp(-L/P)] \tag{19}$$

(see p. 160 in Ref. 31). Three features of the comparison in Fig. 3 should

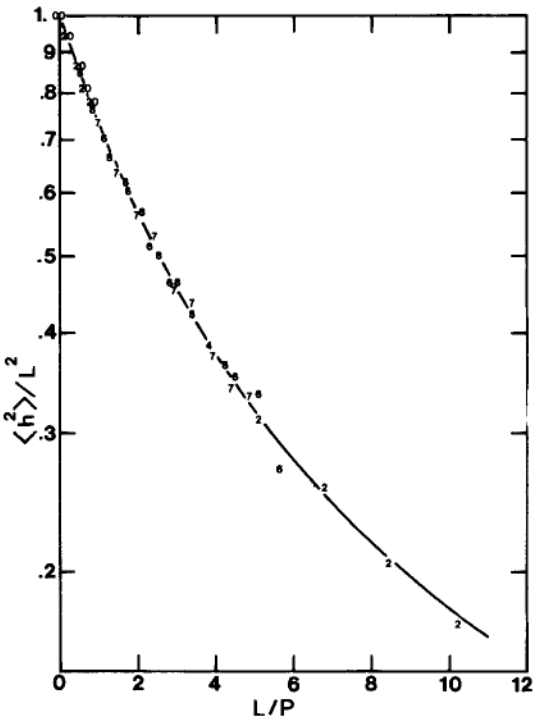

Fig. 3. Comparison of the reduced, mean-squared end-end distance ($\langle h^2\rangle/L^2$) computed for a number of chain ensembles of varying L/P, with the results predicted by Eq. (19) (solid line). The numbers refer to particular values of P in units of 100 Å and represent ensembles of 100–200 chains for each point.

be noted; namely, (1) that the agreement between the ensemble averages and those predicted by Eq. (19) is quite good, (2) that the ensemble averages faithfully represent the predicted averages over a wide range of P values, and (3) that the ensemble sizes (100–200 chains/point) appear to be adequate to describe the true distribution.

Determination of the Rotational Diffusion Coefficients

Approximate Method

For each (L,P) pair chosen for computation, between 100 and 200 chains were generated. The approximate rotational diffusion coefficients ($D_{\hat{\alpha}}$) were computed for each chain by first determining the center of mass, followed by diagonalization of the moment-of-inertia tensor in order to find $\hat{x}$, $\hat{y}$, and $\hat{z}$. The set, $D_{\hat{\alpha}}$, was then computed by using Eq. (13). The ensemble-averaged quantities, $\langle D_{\hat{\alpha}} \rangle$, were determined as outlined above. The results of these computations are plotted in Fig. 4 as the ratio (R_a) of τ_a (the approximate rotational relaxation time, determined from the $\langle D_{\hat{\alpha}} \rangle$) to τ_B [$= 1/6D_B$; determined from Eq. (23), below] as a function of the reduced contour length (L/P). The results have been fit to a cubic equation in X ($= L/P$) using a standard, nonlinear, least-squares curve-fitting routine with the result

$$R_a = 1.0120 - 0.24813X + 0.033703X^2 - 0.0019177X^3 \qquad (20)$$

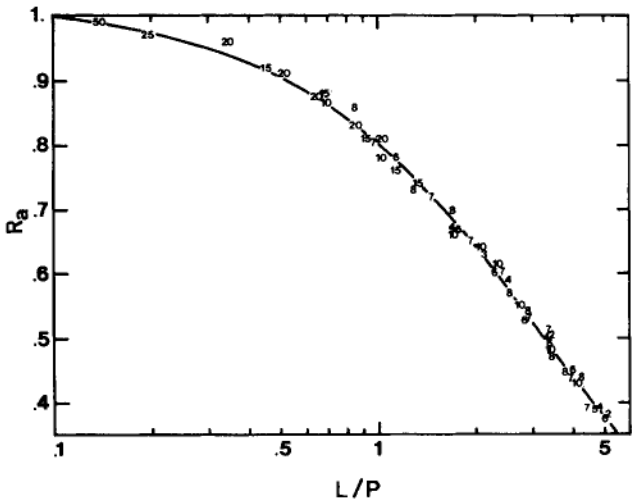

Fig. 4. Plot of $R_a (= \tau_a/\tau_b)$ as a function of the reduced contour length (L/P). τ_a is the approximate rotational relaxation time computed, as described in the text, for ensembles of 100–200 chains. τ_b is the rotational relaxation time of a straight cylinder of axial length, L (volume corrected; see text). The numbers represent P in units of 100 Å. The solid line represents a best-fit, cubic equation [Eq. (20)].

Exact Method

Due to prohibitive requirements for computation time in solving large systems of simultaneous equations for each chain in an ensemble (computing time varies as N^3, and cost varies approximately as N^5; Zimm[13]), a more restricted set of ensembles (20–50 chains/point) were used. For these computations, both exact and approximate rotational diffusion coefficients were determined for each individual chain. The exact rotational diffusion coefficients were determined by first solving Eqs. (9) and (10) for the $F_{i,\alpha}$ by using the ALGOL intrinsics, CHOLDET1 and CHOLSOL1, which employ the Cholesky procedure for solving systems of simultaneous equations. (For details regarding this procedure, see Ref. 13 and references cited therein.) The set, D_p, was then determined from Eqs. (11) and (12). The results of these computations are reported (Fig. 5) as a correction factor (Y) defined by

$$R_c(\text{exact}) = R_a \times (1 - Y) \tag{21}$$

where Y is fitted to

$$Y = 0.06469X - 0.01153X^2 + 0.0009893X^3 \tag{22}$$

The range of validity of the present analysis is given by

$$0.1 < L/P < 5.0, \qquad L/2b > 20$$

The expression for Y includes a constant 1.8% correction in order that

$$\lim_{p \to \infty} \frac{R_a}{R_c} = 1$$

This adjustment is considered somewhat arbitrary (as discussed below) in view of the theoretical uncertainties which exist at this level of precision;

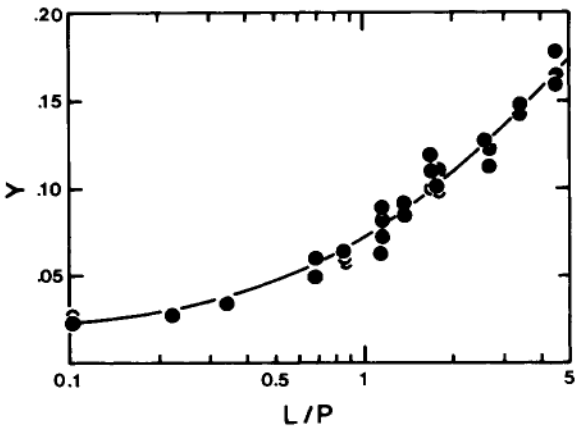

Fig. 5. Plot of the correction factor (Y) required to bring R_a into coincidence with the exact results. Each filled circle represents an ensemble of 20–100 chains, where the exact and approximate hydrodynamic analyses were carried out on a chain-by-chain basis prior to ensemble averaging.

however, the corresponding uncertainty (due to this correction) in P is only 5–6%. Finally, it should be noted (Fig. 4) that R_a is essentially independent of the axial ratio, provided that the conditions of validity stated above are satisfied.

Computational Uncertainties

The aggregate computational uncertainty associated with this analysis is believed to be approximately $0.03R_c$. This value includes contributions from the uncertainty of the rigid-rod limit, as well as the statistical uncertainty associated with the use of finite ensembles. In terms of resultant uncertainties in P, for $1 < L/P \leq 5$ ($0.76 \geq R_c \geq 0.3$), the percent uncertainty in P is approximately constant at ~10%. As L/P decreases below 1, this uncertainty in P increases, largely due to the imprecision of the rigid-rod limit. For example, for $L/P = 0.5$, the uncertainty in P is approximately 20%. For most practical purposes, it is desirable to work at values of $L/P \geq 0.5$.

Computer Facilities

All programs were written in ALGOL and were run on the Burroughs B6700 or an improved system (B7800) on the campus of the University of California, San Diego.

RESULTS AND DISCUSSION

Broersma's Expression for the Transverse Rotational Diffusion Coefficient of a Straight Cylinder Provides a Suitable Standard for the Comparison of Wormlike Chain Models in the Rigid-Rod Limit

At present, the most accurate hydrodynamic analysis of the transverse rotational motion of long cylinders is that of Broersma,[4] who extended Burgers' treatment[3] of the problem and included an analysis of end effects. On the basis of his theoretical and experimental investigations, Broersma arrived at an expression for the rotational diffusion coefficient (D_B); namely,

$$D_B = (3kT/\pi\eta_0 L^3)\{\ln(L/b) - 1.57 + 7[1/\ln(L/b) - 0.28]^2\} \quad (23)$$

where L is the axial length of the cylinder, b is the transverse radius, η_0 is the viscosity of the solvent, k is Boltzmann's constant, and T is the temperature (K). Broersma's expression is believed to be most accurate for rods having axial ratios greater than 10. It should be noted, however, that there is no rigorous theoretical basis for Eq. 23; rather, it represents a "best fit" to both theoretical and experimental results obtained by Broersma. Consequently, the justification for the use of Eq. (23) must rely on exper-

iments. Several investigators[5–7] have reported values for the rotational diffusion coefficient of TMV (axial ratio $\cong$ 20), and the average of these values agrees with D_B to within 2% (Table II). An axial ratio of 20 corresponds to a DNA molecule approximately 150 bp long. The uncertainties associated with the application of hydrodynamic analyses of smooth cylinders to real molecules increase as the axial ratios become smaller, primarily because of end effects. Therefore, the current analysis will only deal with molecules having axial ratios greater than or equal to 20.

In view of the experimental results quoted above, it appears that Broersma's expression yields values for the diffusion coefficients of rigid cylinders which are accurate to within a few percent. Equation (23) should therefore serve as a reasonable representation for the behavior of wormlike chains in the limit, $P \rightarrow \infty$.

Comparison of Several Models Used to Compute the Rotational Relaxation Times of Wormlike Chains

As discussed above, Broersma's expression provides a good representation of the rotational diffusion of straight cylinders. However, at least thus far, continuous models have not been directly applicable to the study of the rotational diffusion of wormlike chains (in the absence of configurational preaveraging) due to the magnitude of the computational task involved. An alternative model, namely, a wormlike chain composed of a string of Stokes' spheres, has been employed by Hearst[12] in an attempt to develop analytical expressions for the rotational diffusion coefficients of wormlike chains. In the weakly-bending-rod (WBR) limit, Hearst obtained

$$D_H(\text{WBR}) = [kT/8\pi\eta_0(nl)^3][3\ln(n) - 0.92 + O(\lambda) + f(\lambda)] \quad (24)$$

($n \gg 1$, $\lambda n \ll 1$) with

$$f(\lambda) = \lambda n(4.5\ln(n) - 6.20) + O(n^{-1}) \quad (25)$$

TABLE II
Rotational Diffusion Coefficients of TMV[a]

Investigator	Method	D_R[b] (sec^{-1})
O'Konski and Haltner (Ref. 5)	TEB[c]	291
Allen and van Holde (Ref. 6)	TEB	298
Newman and Swinney (Ref. 7)	TED	318
Average value		302
Predicted value[d]		308
Difference		2%

[a] These studies have also been included in a larger table of D_R (exp.) values obtained by various methods (see Ref. 7)

[b] Values are corrected to 20°C by the equation $D(20) = D(T)\,(\eta_T/\eta_{20})\,(293/T)$ as determined by Newman and Swinney (Ref. 7).

[c] TEB (transient electric birefringence); TED (transient electric dichroism).

[d] Based on $L = 298 \pm 6$ nm (Ref. 32); and $b = 15$ nm (Ref. 7).

representing the contribution to D_H(WBR) due to chain flexibility. Hearst obtained

$$D_H(\text{WLC}) = (kT/\eta_0)(\lambda/l)^3(1/\lambda n)^2[0.253(\lambda n)^{1/2} + 0.159\ln(1/\lambda) - 0.227 + O(\lambda) + O(\lambda^{-1/2}n^{-1/2})] \quad (26)$$

for long, wormlike chains. Equations (24) and (26) represent the specific case where the bead spacing (l) is equal to the hydrodynamic diameter (2σ); $n = (N-1)/2$; $O(\lambda)$, $O(n^{-1})$, and $O(\lambda^{-1/2}n^{-1/2})$ represent terms of order λ, n^{-1}, and $\lambda^{-1/2}n^{-1/2}$, respectively; and $\lambda = l/2P$. The basic diffusion equation [Eq. (13)] derived by Hearst,[12] from which Eqs. (24) and (26) were derived, was based on the formalism of Kirkwood[16–18] that was later shown to contain some errors, thus reducing its generality. (For a discussion of this point, see Ref. 20, and references therein.) However, Hearst's diffusion equation becomes exact in the rigid-rod limit as $P \to \infty$.[21]

In developing the analytical expressions for the two limiting cases mentioned above [Eqs. (24) and (26)], two additional mathematical operations were employed. The first operation nvolved preaveraging over configuration space in order to facilitate the subsequent analysis. This procedure is quite often employed in treatments of the hydrodynamics of flexible chains; however, Zimm[13] has shown that in computing the intrinsic viscosity and sedimentation coefficients of Gaussian chains, the preaveraging assumption leads to errors of 12 and 13%, respectively. Furthermore, Yamakawa[19] has pointed out that configurational preaveraging eliminates certain correction terms applied to the Oseen-Burgers hydrodynamic interaction tensor. The second operation employed by Hearst involved the replacement of the double sums in Eq. (13) by integrals, in order to facilitate the development of analytical expressions for the two cases mentioned above. For chains composed of a relatively small number of beads, however, the integral approximation is expected to lead to significant errors[33] (see Discussion below).

Rigid-Rod Limit

One important requirement of any hydrodynamic model for a wormlike chain is that it yield the same rotational relaxation times in the rigid-rod limit as those predicted from the continuous cylinder model of Broersma. In Fig. 6, R ($= \tau/\tau_B$) is plotted as a function of the axial ratio ($L/2b$); several features should be noted.

1. Curves 1 and 2, representing the limiting form of Hearst's analytical expression [Eq. (24)] for the weakly bending rod, overshoot ($R = \tau/\tau_B = D_B/D_H(\text{WBR}) > 1$) the corresponding values predicted by Eq. (23) (D_B) by approximately 9 and 7%, respectively, for the largest axial ratios. The origin of this discrepancy is not completely understood but may be due, in part, to the application of integral approximations by that author (see below).

2. The approximation to the continuous cylinder model, in which the

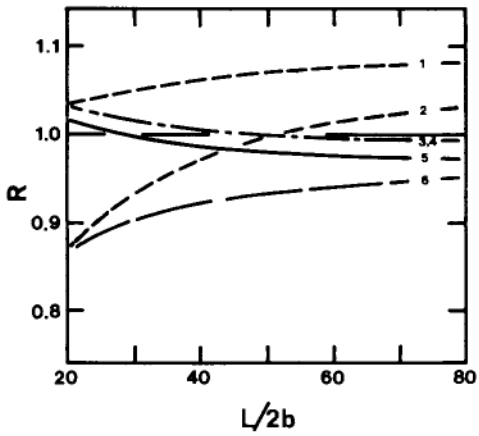

Fig. 6. Comparison of the computed rotational relaxation times, plotted as $R(=\tau/\tau_b)$ versus the axial ratio $(L/2b)$ of a volume-corrected cylinder (see text) for various hydrodynamic models in the rigid-rod limit. Curves: 1, weakly-bending-rod (WBR) model of Hearst (Ref. 12), Eq. (26); 2, WBR model, as in 1, except that there are $N-1$ beads; 3, wormlike-chain model employing the diffusion equation of Hearst [Eq. (13)]; 4, same as 3, except that there are $N-1$ beads, and the beads have been spaced at equal distances along the chain such that the terminal beads are in the same locations as would be the case for N beads (nontouching model; approaches the touching model as $N \to \infty$); 5, model equivalent to that used in 3, except that the formal solution to the coupled hydrodynamic equations has been carried out as described in the text; 6, $N-1$ touching beads, computed as in curves 3 and 4. Curve 4 has not been plotted separately, since it overlaps curve 3 (<0.2% difference). The difference between curves 3 and 5 varies by less than 0.2% over the range studied.

ends of the terminal beads are at the same positions as the ends of the cylinder (curve 6), significantly underestimates the hydrodynamic resistance for small axial ratios, as expected from Broersma's study.[4]

3. Placement of the centers of the terminal beads at the ends of the continuous cylinder (curve 3) markedly improves the agreement between the bead and continuous cylinder models; however, curves 3 and 6 eventually converge (difference $< 1\%$ for $L/2b > 130$).

4. Removal of a single bead from the interior of the chain has very little effect on the hydrodynamic resistance (reducing R by approximately 0.1%; curve 4, not plotted separately) as long as the terminal beads remain in the same locations as for curve 3.

5. Curve 5, representing the formal solution to the hydrodynamic problem, differs from curve 3 by approximately 1.8%. This difference varies by less than 0.3% over the entire range of axial ratios investigated in this study. The correction factor (Y) has been adjusted by 1.8% in order to bring the limiting results for R_a into correspondence with R_c. As mentioned above, this adjustment is somewhat arbitrary in view of the uncertainty in the verification of Broersma's expression at this level of precision; however, the attendant uncertainty in P is rather small. Moreover, it should be noted that the form of the hydrodynamic interaction tensor [Eq. (5)] used in this analysis is itself somewhat approximate; the

justification for its use (as well as the volume-corrected model itself) being that it yields a rigid-rod limit that is within a few percent of the experimentally verified, continuous-cylinder model developed by Broersma.

Moderately Stiff, Wormlike Chains

Figure 7 displays the results of several hydrodynamic models, the details of which are given in the legends to Figs. 6 and 7. The expression [Eq. (26)] derived by Hearst [D_H(WBR)] yields values of R which are substantially larger than corresponding results for either the basic diffusion equation [Eq. (13); curve 2] or the more formal analysis (curve 3). This difference can, in part, be rationalized in terms of the approximations made by that author. In particular, the use of approximate integral solutions should introduce significant errors for small values of n, and the extent to which this approximation contributes to the difference between curve 1 and curve 2 or 3 can be appreciated by inspection of Fig. 8. Hearst has pointed out that Eq. (26) is only valid for $n \gg 1$; the analysis presented in Fig. 8 provides a more quantitative assessment of this criterion.

One approximate model, represented by curve 4, involves the use of the

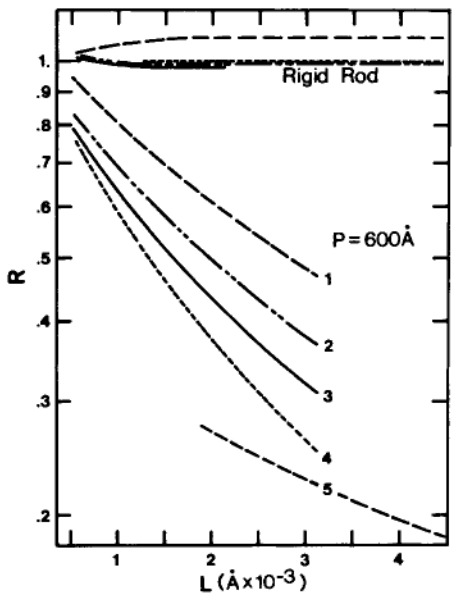

Fig. 7. Comparison of the computed rotational relaxation times, plotted as in Fig. 6, for several wormlike-chain models, corresponding to the limiting forms described in the legend to Fig. 6. In all cases, the chains are composed of N beads ($N - 1$ segments). Curves: 1, WBR model of Hearst, Eq. (24); 2, wormlike-chain model, employing the approximate diffusion equation of Hearst [Eq. (13)]; 3, the formal hydrodynamic analysis; 4, equivalent (Broersma) cylinder model described in the text; 5, long-wormlike-chain model of Hearst [Eq. (26)]. $b = 13$ Å. The rigid-rod limits corresponding to curves 1–4 are represented in the upper portion of the figure.

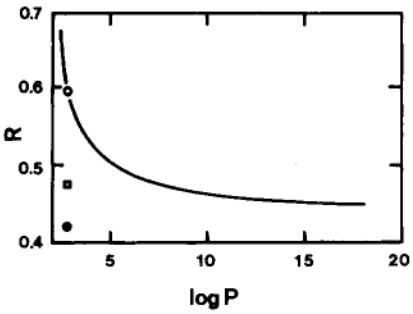

Fig. 8. Dependence of Hearst's WBR formula [Eq. (24)] on the number of beads comprising the chain. Actual plot is of R for a chain of $L/P = 3.4$, as a function of P. The symbols ○, □, and ● represent the corresponding points on Fig. 7 for curves 1, 2, and 3, respectively.

rms end-to-end length ($\langle h^2 \rangle^{1/2}$) as an effective cylinder length in Broersma's expression [Eq. (25)]. In this example, the "radius" of the cylinder has been adjusted so that the effective cross-sectional area of the equivalent cylinder is the same as that of the original wormlike chain. In view of the simplistic nature of this model, the agreement with the formal analysis (curve 3) is surprisingly good.

Flexibility of Wormlike Chains Can Be Determined in the Absence of a Precise Knowledge of the True Hydrodynamic Radius

In most studies of the hydrodynamic properties of wormlike chains, the assumption is made that the local molecular cross section can be effectively represented by an equivalent (circular) cross section. Furthermore, in choosing an effective hydrodynamic radius, assumptions are invariably made regarding the draining properties of the solvent and associated counterions in the vicinity of the macromolecule. For example, in the analysis of the rotational diffusion of DNA presented in the following article,[11] the value of 13 Å has been chosen as the effective hydrodynamic radius (b). Implicit in this choice is the assumption that the solvent in the major and minor grooves is essentially nondraining. This nondraining assumption is a standard one and is based on both theoretical[4,34,35] and experimental[4] studies. For polyelectrolytes, an additional uncertainty exists in that closely associated counterions may contribute to the effective hydrodynamic radius (see Ref. 11). However, provided that the length of the polymer is known, information pertaining to the flexibility of the polymer can be obtained in the absence of a precise knowledge of b, as will be shown below.

If an assumed value of b differs from the true hydrodynamic radius (b_T), then

$$R_c(b) = \frac{R_c(b_T)}{f(b/b_T, L)} \tag{27}$$

where $R_c(b)$ is determined from measurement and an assumed value for b, and where

$$f(b/b_T,L) = \tau_B(b)/\tau_B(b_T) = D_B(b_T)/D_B(b) \tag{28}$$

[Eq. (23)]. The uncertainty associated with b can be substantially reduced by determining $R_c(b)$ for a series of fragments of varying length, and by noting that

$$\frac{\partial \ln[R_c(b)]}{\partial L} = \frac{\partial \ln[R_c(b_T)]}{\partial L} - \frac{\partial \ln(f)}{\partial L} \tag{29}$$

The assumed value of b can be varied until Eqs. (27) and (29) are consistent with a single value of P. It should be noted (Fig. 9) that f is only slightly dependent on L. For example, if the initial choice for b differs from b_T by less than 20%, f varies by less than 3% over a fivefold range of L. As an added bonus, this analysis should provide a reasonably accurate estimate for b_T. In principle, an approach entirely analogous to the one presented above could be taken if the hydrodynamic radius of the polymer were known; however, this latter situation is rarely experienced in practice.

The most general (and most frequent) situation involves a lack of a precise knowledge of either the length (or length per monomer) or the hydrodynamic radius of the polymer. In this case, a more general analysis can be performed by imposing the constraint that P is independent of L. This constraint follows directly from the basic properties of the isotropic wormlike chain. This latter approach will be discussed in detail in the following paper.[11]

Applicability of the Equilibrium-Ensemble Approach to the Study of the Diffusion of Wormlike Chains

In the present analysis it has been assumed that the behavior of a flexible wormlike chain undergoing pure rotational diffusion can be effectively

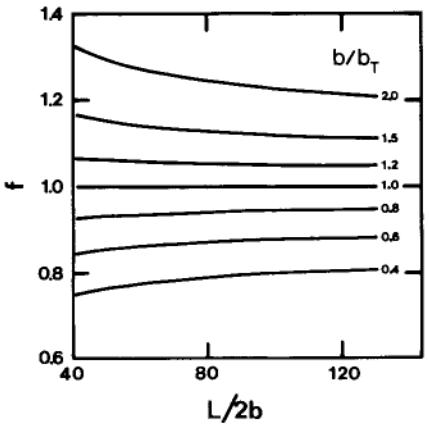

Fig. 9. Plot of $f(b/b_T,L)$ as a function of L for rigid cylinders having various assumed radii (b), compared to a standard value (b_T).

described at any instant by a collection of chains having an ensemble-averaged configuration identical to the time-averaged configuration of the original chain and whose individual friction tensors are given by the instantaneous, frozen configurations of each chain in the ensemble. This assumption has been almost universally applied to the study of the hydrodynamics of flexible chains (for example, see Refs. 12, 33, 36, 37), and is based, in part, on the work of Kramers,[38] who concluded that the diffusion problem could be solved correctly using the rigid-body approach (Kramers neglected hydrodynamic interactions). The Kirkwood formalism[16] is based on this approach.

One of us showed some time ago[39] that the Kirkwood-Riseman results for the viscosity number of Gaussian chains at small velocity gradients could be obtained independently of whether the chains were assumed to be flexible or rigid, and Gotlib and Svetlov[40] later showed that this was still true for chains with an arbitrary intersegment interaction potential. However, in both cases the hydrodynamic interaction tensor was preaveraged.

The studies referred to above all suggest that an ensemble of flexible polymers undergoing rotational or translational motion can at least sometimes be treated as an equivalent ensemble of instantaneously rigid chains. In the absence of a complete hydrodynamic analysis of flexible polymers—one that considers a general intramolecular potential, as well as intramolecular hydrodynamic interactions, and avoids preaveraging (perhaps through a dynamical approach)—the above conclusion must remain nonrigorous. However, any subsequent modification of the above conclusion is expected to introduce only second-order corrections to the present analysis.

It has also been assumed that the segmental motions of the wormlike chain are more rapid than is overall rotational diffusion, thus allowing the use of ensemble-averaged rotational diffusion coefficients to describe the orientational relaxation process. This assumption can be at least approximately validated for short chains by computing the relaxation spectrum for transverse motions, using the formula derived by Barkley and Zimm[41] (which includes intrachain hydrodynamic nteractions); namely,

$$\tau_k' = 4\pi\eta_0/kTP\kappa_k^4[K_0(\kappa_k b) + (\kappa_k b/2)K_1(\kappa_k b)] \tag{30}$$

where τ_k' is the bending relaxation time of the kth normal mode, κ_k is the wave number [satisfying the relation, $\cos(\kappa L)\cosh(\kappa L) = 1$], b is the cylinder radius, P is the persistence length, and η_0 is the solvent viscosity, and where $K(\kappa b)$ are modified Bessel functions. This formula is approximate in the present context (for small values of k) in that it employs harmonic wave functions and neglects end-effect corrections to the intrachain hydrodynamic interactions. In the range of validity of this formula ($L < P$), the longest transverse (bending) relaxation time (τ_1') is much faster than the

corresponding rotational relaxation time for the wormlike chain (roughly one order of magnitude shorter for $L = P$). For chains of $L > P$, no adequate description exists for the internal motions of the wormlike chain; however, the schematic "correlation diagram" of Stockmayer[42] can be used as a rough guide. It suggests that the fundamental bending mode of the weakly bending rod correlates with the second (triply degenerate) relaxation time for the random coil, which is approximately three times shorter than the first (longest) relaxation time.[39,43] As for the "rigid-chain" assumption discussed above, this approach must remain nonrigorous (for chains of $L > P$) in the absence of a proper analysis of the internal motions of moderately flexible wormlike chains; however, in view of the above discussion, it is plausible to assume that a substantial amount of segmental motion occurs on the time scale of overall rotational diffusion and, therefore, that an ensemble-averaged rotational relaxation time adequately represents the rotational diffusion of short wormlike chains.

It is, however, instructive to consider the other extreme case, namely, the rotational diffusion of an ensemble of wormlike chains having internal coordinates that are fixed on the time scale of rotational relaxation. For this case, the relaxation of the optical anisotropy would represent a superposition of a continuum of relaxation processes corresponding to the various relaxation times for the individual chains (Table I), weighted according to the configurational distribution as well as the contribution of each configuration to the overall optical anisotropy. For this static model, the terminal portion of the decay curve represents the weighted contributions from the most extended chains. Therefore, the application of the ensemble-averaged model to molecules which are not undergoing rapid (compared to rotation) segmental motions would lead to an overestimate of the true persistence length.

Effects of Coupling Between Rotational and Translational Motions

In assuming that individual wormlike chains experience pure rotational motion, effects due to the coupling of translational and rotational motions[44,45] have been neglected. Since individual chains usually manifest a rather low degree of symmetry, coupling is expected to occur; however, for the wormlike chains considered in this analysis, the influence of such coupling on rotational diffusion is not significant. For example, in computing the apparent rotational diffusion coefficients (which include contributions from coupling) for an ensemble of 10 chains ($L/P = 2$), the contribution due to coupling was found to be less than one part per thousand for the ensemble, and less than three parts per thousand for any individual chain (Hagerman and Zimm, unpublished work). An occasional chain may possess a fair degree of helicoidal symmetry, thus leading to a significant degree of coupling[44]; however, such chains are rare and do not contribute significantly to the properties of the ensemble.

CONCLUSIONS

The foregoing analysis has provided a means by which the rotational diffusion of moderately flexible polymers can be quantitatively related to their persistence lengths. The rotational relaxation times of these polymers are extremely sensitive to changes in configuration, and studies of the behavior of these relaxation times should prove to be a powerful approach for the investigation of the influence of various agents (solvent composition, ionic strength, ligand binding, etc.) on polymer flexibility. Furthermore, since molecules can be studied in a size range where excluded-volume effects are negligible ($L/P < 5$) (see Ref. 11), the uncertainties involved with this latter effect have been removed.

In addition, the persistence lengths of polymers having local hydrodynamic radii that are not known precisely can still be determined with reasonable accuracy by studying the rate of departure (as a function of increasing L) of the observed rotational relaxation times from those expected for rigid cylinders having the same axial length. Moreover, this approach should yield a reasonable estimation of the hydrodynamic radius.

Finally, the exploitation of the full sensitivity of this analysis demands a precise knowledge of the axial lengths of the polymers being investigated. For DNA, this condition can be satisfied by using restriction fragments which have been entirely sequenced.[11] However, if changes in flexibility and/or local structure are under investigation, without regard to absolute values of P, then the method is equally applicable to systems where precise length information is not available.

The authors wish to thank Dr. J. Hearst for providing unpublished material, and Dr. W. H. Stockmayer for discussions in connection with Ref. 41. This research has been supported by a grant (GM 11916) from the National Institutes of Health (B.H.Z.), and by a Leukemia Society of America postdoctoral fellowship (P.J.H.). The research was performed at U.C.S.D.

References

1. Perrin, F. (1934) *J. Phys. radium* **5,** 497–511.
2. Perrin, F. (1936) *J. Phys. radium* **7,** 1–11.
3. Burgers, J. M. (1938) *Second Report on Viscosity and Plasticity*, Amsterdam Academy of Science, Nordemann, Amsterdam.
4. Broersma, S. (1960) *J. Chem. Phys.* **32,** 1626–1631.
5. O'Konski, C. T. & Haltner, A. J. (1956) *J. Am. Chem. Soc.* **78,** 3604–3610.
6. Allen, F. S. & van Holde, K. E. (1971) *Biopolymers* **10,** 865–882.
7. Newman, J. & Swinney, H. L. (1976) *Biopolymers* **15,** 301–315.
8. Ding, R. -W., Rill, R. & van Holde, K. E. (1972) *Biopolymers* **11,** 2109–2124.
9. Hogan, M., Dattagupta, N. & Crothers, D. M. (1978) *Proc. Natl. Acad. Sci. USA* **75,** 195–199.
10. Stellwagen, N. (1981) *Biopolymers* **20,** 399–434.
11. Hagerman, P. J. (1981) *Biopolymers* **20,** 1503–1535.
12. Hearst, J. (1963) *J. Chem. Phys.* **38,** 1062–1065.
13. Zimm, B. H. (1980) *Macromolecules* **13,** 592–602.
14. Garcia de la Torre, J. & Bloomfield, V. A. (1977) *Biopolymers* **16,** 1747–1763.

15. Schellman, J. A. (1974) *Biopolymers* **13,** 217–226.
16. Kirkwood, J. G. & Riseman, J. (1948) *J. Chem. Phys.* **16,** 573–579.
17. Kirkwood, J. G. (1954) *J. Polym. Sci.* **12,** 1–14.
18. Riseman, J. & Kirkwood, J. G. (1956) *Rheology*, Vol. 1, Academic Press, New York.
19. Yamakawa, H. (1970) *J. Chem. Phys.* **53,** 436–443.
20. Garcia de la Torre, J. & Bloomfield, V. A. (1977) *Biopolymers* **16,** 1765–1778.
21. Yamakawa, H. & Yamaki, J. (1973) *J. Chem. Phys.* **58,** 2049–2055.
22. Wegener, W. A., Dowben, R. M. & Koester, V. J. (1979) *J. Chem. Phys.* **70,** 622–632.
23. Tao, T. (1969) *Biopolymers* **8,** 609–632.
24. Ehrenberg, M. & Rigler, R. (1972) *Chem. Phys. Lett.* **14,** 539–544.
25. Sherwood, D. H. (1974) Thesis, University of California, San Diego.
26. Ridgeway, D. (1966) *J. Am. Chem. Soc.* **88,** 1104–1112.
27. Ridgeway, D. (1968) *J. Am. Chem. Soc.* **90,** 18–22.
28. Benoit, H. (1951) *Ann. Phys.* **6,** 561–609.
29. Knuth, D. E. (1969) *The Art of Computer Programming*, Vol. 2, Addison-Wesley, Menlo Park, Calif.
30. Eyring, H. E. (1932) *Phys. Rev.* **39,** 746–748.
31. Bloomfield, V. A., Crothers, D. M. & Tinoco, I. (1974) *Physical Chemistry of Nucleic Acids*, Harper & Row, New York.
32. Hall, C. E. (1958) *J. Am. Chem. Soc.* **80,** 2556–2557.
33. Yamakawa, H. & Fujii, M. (1973) *Macromolecules* **6,** 407–415.
34. Bloomfield, V. A., Dalton, W. D. & van Holde, K. E. (1967) *Biopolymers* **5,** 135–148.
35. McCammon, J. A., Deutch, J. M. & Felderhof, B. U. (1975) *Biopolymers* **14,** 2613–2623.
36. Hearst, J. E. & Stockmayer, W. H. (1962) *J. Chem. Phys.* **37,** 1425–1433.
37. Yamakawa, H. & Fujii, M. (1974) *Macromolecules* **7,** 128–135.
38. Kramers, H. A. (1946) *J. Chem. Phys.* **14,** 415–424.
39. Zimm, B. H. (1956) *J. Chem. Phys.* **24,** 269–278.
40. Gotlib, Yu. Ya. & Svetlov, Yu. Ye. (1966) *Vysokomol. Soyed.* **8,** 1517–1523 [(1966) *Polym. Sci. USSR* **8,** 1670–1677].
41. Barkley, M. D. & Zimm, B. H. (1979) *J. Chem. Phys.* **70,** 2991–3007.
42. Stockmayer, W. H. (1973) in *Molecular Fluids*, Balian R. & Weill, G., Eds., Gordon and Breach, New York.
43. Zimm, B. H., Roe, G. M. & Epstein, L. F. (1956) *J. Chem. Phys.* **24,** 279–280.
44. Brenner, H. (1955) *J. Colloid Sci.* **20,** 104–122.
45. Brenner, H. (1967) *J. Colloid Interface* **23,** 407–436.

Received October 17, 1980
Accepted January 21, 1981